Experiments and direct numerical simulations of two-dimensional turbulence

C. H. Bruneau[1] and H. Kellay[2]
[1]*Mathématiques Appliquées de Bordeaux, Université Bordeaux 1, 351 cours de la Libération, 33405 Talence cedex, France*
[2]*Centre de Physique Moléculaire Optique et Hertzienne (UMR 5798), Université Bordeaux 1, 351 cours de la Libération, 33405 Talence cedex, France*
(Received 23 December 2003; revised manuscript received 23 July 2004; published 25 April 2005)

Experiments and direct numerical simulations reveal the coexistence of two cascades in two-dimensional grid turbulence. Several features of this flow such as the energy density and the scalar spectra are found to be consistent with well known theoretical predictions. The energy transfer function displays the expected upscale energy transfers. The vorticity correlation function is logarithmic and thus consistent with recently proposed models.

DOI: 10.1103/PhysRevE.71.046305 PACS number(s): 47.27.−i, 47.11.+j

Two-dimensional (2D) turbulence is believed to be important for the understanding of large scale atmospheric and oceanic flows and is of fundamental importance for the understanding of turbulence in general [1]. The two-dimensionality affects several features of the flow including its mixing properties which are important for industrial and natural processes. Two-dimensional turbulence admits two different inertial ranges. This scenario as well as the scaling laws for the two regimes were worked out more than 30 years ago by Kraichnan and Bachelor [2]. The first range is at smaller scales than the injection scale and is supposed to be host to a direct enstrophy (squared vorticity) cascade from the large to the small scale. The second range is at larger scales than the injection scale and is host to an inverse energy cascade from the small to the large scale. Some doubts persist, however, as to the validity of such a picture at low Reynolds numbers [3].

Experimental and numerical evidence for the coexistence of the two cascades is scarce (see [4] for a review) and an important step has been carried out by Rutgers [5] who demonstrated that such a situation can be obtained in turbulent soap films [4]. We here follow a slightly modified scheme to obtain such a flow and characterize its properties in both experiments and direct numerical simulations (DNS). We focus on previously unmeasured quantities such as the energy transfer function, the scalar spectrum, and the vorticity correlation functions. Our results are consistent with theoretical expectations for the velocity (or energy spectra) and the energy transfer function which is notoriously difficult to measure. Results for the passive scalar dispersion are also in agreement with these predictions. The vorticity correlation function shows the expected logarithmic variation.

The experiments use rapidly flowing soap films where the flow is perturbed by arrays of small cylinders. The experimental techniques used are laser Doppler velocimetry (LDV) for the measurement of the velocity or vorticity fluctuations and interferometry for the measurement of thickness fluctuations [4,6]. The velocity measurements are taken in two points (using two LDV probes separated by a small horizontal distance between 0.3 and 0.7 mm depending on the data rate of the LDV) to estimate the vorticity using the Taylor hypothesis [4]. For both measurements, the time trace of the signal is recorded and the Taylor hypothesis is used to convert time scales to length scales. This hypothesis has been thoroughly tested in such flows [7] and assumes that the flow structures are convected past the observation point without much deformation. The DNS benefit from recent advances in the calculation of 2D flows around circular obstacles and use a so called penalization scheme which assimilates the obstacles to porous media whose permeability can be made very small [8]. The resolution for the simulations was 640×2560. In the DNS, the measurements were also made at particular locations and time traces were recorded just as in experiments so that comparisons can be made with no further assumptions. More information on the numerical techniques and the experimental techniques can be found in several references [4,6,8]. Briefly, the soap films are suspended on vertical nylon wires such that the flow is driven by gravity. The mean longitudinal velocities obtained hover at around 2 m/s and the turbulence intensity can be as high as 15% in experiments and even higher for the simulations as they reach higher Reynolds numbers. The films obtained can last several hours as they are replenished at the top of the channel by soap water using a small micropump delivering a volume flux between 0.05 and 1 ml/s. As the flux increases, the mean velocity, the turbulent intensity, and the mean thickness of the film increase. The flux is therefore the control parameter for the experiments. The results reported here are basically taken at a flux of 0.4 ml/s for which a mean velocity of 1.6 m/s is achieved with a turbulence intensity of 10%. The mean thickness of the film is 5 μms with a standard deviation of less than 5% [6].

The experiments and the DNS use a 2D channel where the flow is perturbed by arrays of cylinders placed both horizontally and vertically. The width of the channel, W, is 5 cm for the experiments and 1 for the simulations. In units of channel width, the diameter of the five cylinders in the horizontal array was 0.1 with a spacing of 0.2. The diameter of the cylinders in the two vertical arrays placed at 0.1 from the channel walls was 0.04 for the experiments and 0.02 for the simulations; the spacing between the cylinders was 0.2. This geometry is shown in Fig. 1 along with a snapshot of the vorticity field and the thickness field for the simulations and the experiments, respectively. The presence of the cylinders

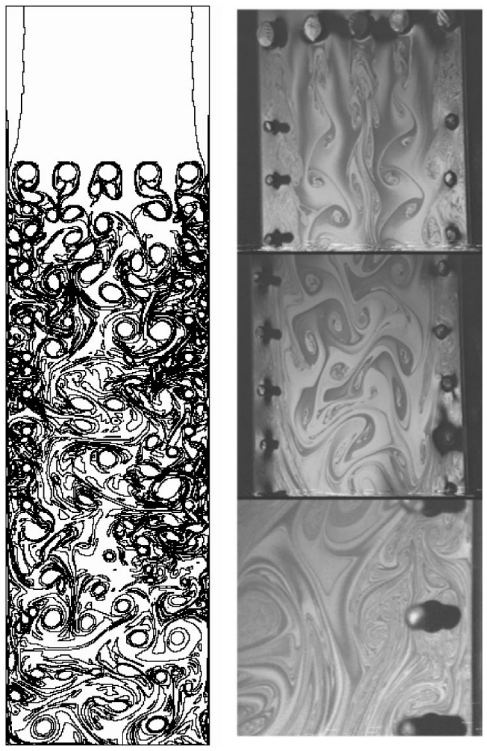

FIG. 1. Left: vorticity field from DNS (Re=5000). Right: photos near the first horizontal grid and further downstream in the soap film channel. Third photo: a zoom on the side of the channel to show the intense activity created by the vertical cylinders in the soap film.

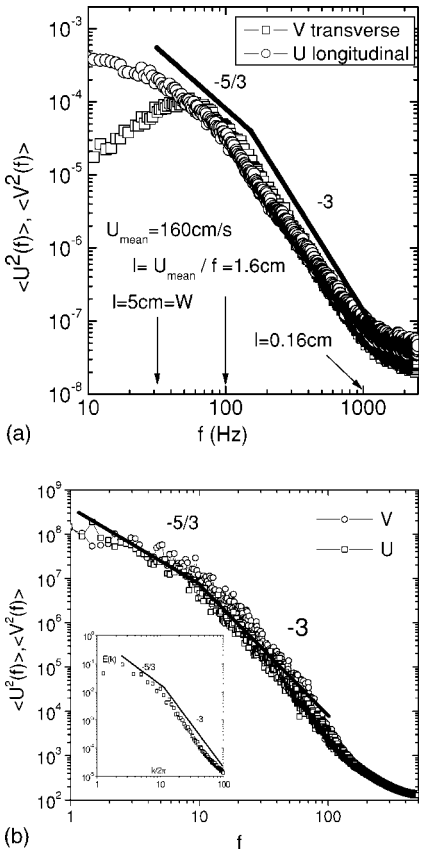

FIG. 2. Power spectra from experiments (a) and simulations (b) for the velocity (longitudinal U and transverse V). The velocity spectra and the energy density are shown in arbitrary units. The frequency axis and the wave-number axis in (b) and the inset to (b) are in reduced units in such a way that a frequency f of 1 and a value of 1 for $k/2\pi$ correspond to the channel width. Inset of (b): Energy density spectrum obtained from the spatial velocity field for the DNS. The frequency axis in the experimental data can be converted to length scales using the frozen turbulence assumption (in units of channel width): 160 Hz corresponds to $1/5$ (or 1 cm in physical units). For the numerics the same thing can be achieved: $f=10$ corresponds to $1/10$ (in units of channel width).

on the sides of the channel clearly makes for the injection of small scale vorticity into the main flow. This is very different from the situation where only the horizontal grid is present for which previous experiments and numerical simulations evidenced an enstrophy cascade only [9,4,8]. Measurements were taken at different positions from the horizontal grid in the central region of the channel. While near the horizontal grid only one range is observed, as in previous experiments using only the horizontal grid, farther downstream, clearly two ranges coexist for the velocity spectra. Figures 2(a) and 2(b) shows the power spectra of the two components of the velocity from the experiments (at a distance of 4 from the grid) and the simulations (at a distance of 2.5 from the grid). The first range at large scales is consistent with a $-5/3$ scaling law while the second range is consistent with a -3 scaling exponent. These two ranges are separated by a scale of about $1/10$ for the simulations and between $1/3$ and $1/4$ for the experiments; this is due to differences in Reynolds numbers. The Reynolds number (based on the radius of the horizontal cylinders) for the simulations was 50 000 for the results presented but tests with 5000 and 10 000 were also carried out. The crossover between the two regimes is at $1/4$ and $1/6$ for the two Reynolds numbers, respectively. For the experiments the Reynolds number is rather small and is at best around 5000. However, since the viscosity of the soap film, which is not known directly, can be higher than that of the bulk soap solution, this number can be even smaller. We believe that the quality of the $-5/3$ scaling law at large scales which is relatively poor (half a decade) is due to the small value of the experimental Reynolds number which limits the range of the inverse cascade. This range is naturally limited by the channel width at large scales and by the crossover scale between the two regimes which goes to smaller scales when the Reynolds number increases, as the simulations show. This is not the case for the simulations, which reach much higher values of the Reynolds number and for which the quality of the $-5/3$ regime as well as the isotropy of the flow at large scales is quite good and extends for almost a full decade. For the experiments, the turbulence becomes anisotropic at the large scales, comparable to the channel width. At the small scale end of the spectra, a flattening is seen: for the experiments, this is due to the limited dynamic range of the LDV measurements; for the DNS, this is due to a limitation of the spatial resolution. Besides differences in Reynolds number, the experiments and the DNS also differ in one important aspect, which is the air drag that

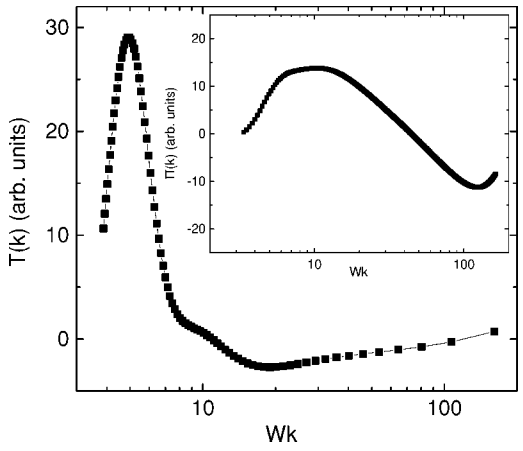

FIG. 3. Energy transfer function $T(k)$ from the experiments; W is the channel width of 5 cm. Inset: the energy flux $\Pi(k)$.

is present in the experiments and absent in the numerics. Its inclusion in the numerical simulations is under way to better understand its effect. The inset to Fig. 2(b) shows the energy density for the numerical simulations calculated in real space directly. The spatial velocity field from a 512×512 window at the base of the channel was Fourier analyzed and averaged over the angle. The result from an average over several images is consistent with the presence of two ranges in agreement with the spectra from the temporal signal which uses the Taylor hypothesis. These results are also in agreement with previous experiments and simulations [5,10,11]. These spectra suggest that the coexistence of two scaling regimes is possible with such a channel flow. The DNS results bring in additional support in the sense that only molecular viscosity is used here with no large scale dissipation.

As mentioned earlier, the energy cascades to large scales in two-dimensional turbulence. A direct test of the direction of energy transfers comes from the energy transfer function $T(k)$ whose origin is the nonlinear term in the Navier-Stokes equations $[\partial E(k)/\partial t = T(k) + \nu k^2 E(k)$, where ν is the kinematic viscosity] as has been demonstrated for 3D turbulence [12]. This function can be calculated from a knowledge of the two correlation functions $S_{111}(r)=\langle u^2(y)u(y+r)\rangle$ and $S_{212}(r)=\langle v(y)u(y)v(y+r)\rangle$ (v is the transverse velocity and r is parallel to u). Van Atta [12] calculated this function for two dimensions and it reads $T(k) = -2k/\pi^2 \int_k^\infty \int_0^\infty r S_{i1i}(r)\cos(k_1 r)dr\, k_1 dk_1/\sqrt{k_1^2-k^2}$ ($i=1,\ 2$). To our knowledge, no experimental measurements of this function, in 2D turbulence, have been carried out so far despite its importance. As can be seen in Fig. 3, $T(k)$ is positive at small k and then swings negative at large k or smaller scales with a small plateau at intermediate scales. The maximum of the positive bump is close to the channel width while the minimum of the negative bump is near 1.5 cm which is near the position of the crossover from the enstrophy to energy cascade range. The $-5/3$ range is situated between these two length scales as expected. Measurements of $T(k)$ in three-dimensional turbulence exhibit the opposite trend: a negative bump at large scales followed by a positive bump at small scales, indicating a direct energy transfer to the small scale end of the spectrum. It must be noted here that an energy inertial range shows up as a flat (very close to zero) part in $T(k)$. However, very few experiments if any (in 3D) have evidenced this. In our case only a small plateau appears; this is certainly due to the small extent of the inertial range and the low value of the experimental Reynolds number.

The shape of $T(k)$ in Fig. 3 directly gives the sense of energy transfers, i.e., from the small to the large scales. A simple way to view this result is that the large scales are gaining energy since the rate of change of the energy density is positive. However, the small scales are losing energy as the rate of change of the energy density is negative. To be more rigorous, however, one needs to evaluate the energy flux $\Pi(k)=\int_0^k T(k)dk$. This function is displayed in the inset to Fig. 3 as a function of Wk. The energy flux is positive and roughly constant at scales where $T(k)$ is flat and close to zero (i.e., for scales between the channel width and the crossover between the two regimes described above). This is the hallmark of the inverse energy cascade as expected for two-dimensional turbulence and as has been shown through previous numerical simulations [13]. The energy flux is therefore roughly constant and positive for the range where a scaling consistent with inverse energy cascade is present. The energy flux then decreases at smaller scales and swings negative in the range where a scaling consistent with an enstrophy direct cascade is present. At even smaller scales, the energy flux goes through a negative minimum and starts to climb up to zero. Scales much smaller than the location of this minimum are, however, not resolved in the experiments here so the full return to zero is not seen.

A third quantity for which our measurements indicate a nice agreement with the theoretical expectations and for which to our knowledge no measurements have appeared in such a situation are the scalar field fluctuations: the thickness of the soap film and its fluctuations around the mean. Their measurement is quite delicate but can be done using a recently developed interferometer [6,14]. As the photographs of Fig. 1 show, the thickness field seems to follow the flow and gives a natural visualization of the vortical structures that detach from the cylinders. Previous measurements of the thickness fluctuations in such soap films [6,14] for decaying turbulence evidenced only one range. Here the measurements are consistent with the coexistence of two scaling regimes just as in the velocity or energy spectra. Indeed, the power spectrum of the soap film thickness fluctuations turns out to be consistent with theoretical expectations for a passive scalar (the expected scaling exponents are $-5/3$ and -1, respectively [13]) as seen in Fig. 4 which shows a $-5/3$ scaling regime at large scales followed by a -1 (with a logarithmic correction) scaling regime at small scales. The two regimes are highlighted with straight lines indicating the $-5/3$ exponent and a regime consistent with a $[k\log_{10}(k/k_0)]^{-1}$ regime. Logarithmic corrections are expected in the enstrophy cascade range [15] so the exponent measured is not -1 exactly. Our results seem to be consistent with such deviations.

To further explore this turbulent flow we have measured the vorticity fluctuations as well. It must be noted here that theoretical calculations and predictions concern the vorticity correlation function or moments of vorticity increments di-

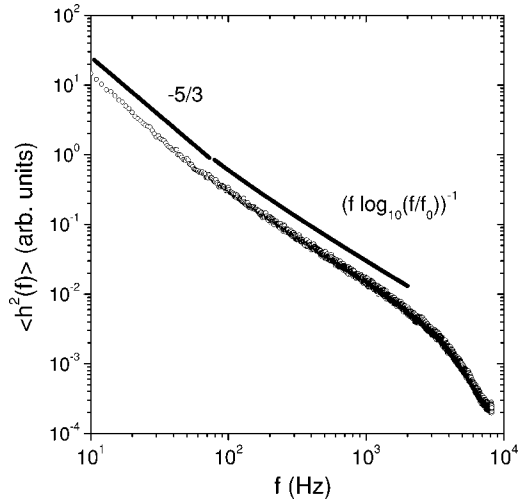

FIG. 4. Power spectrum of thickness fluctuations. $U_{\text{mean}} = 160$ cm/s so 100 Hz corresponds to 1.6 cm.

rectly rather than the spectrum. One of the main predictions states that the vorticity (ω) correlation function, or more precisely, $\langle\omega(0)\omega(r)\rangle^{3/2}$ is logarithmic in r [15]. In Figs. 5(a) and 5(b) we test the validity of the logarithmic correction where $\langle\omega(0)\omega(r)\rangle^{3/2}$ is displayed versus the increment r. To a good approximation, this correlation function is logarithmic in r. From this figure we conclude that the logarithmic correction is relevant for both the experiments and the simulations. The second order structure functions of the vorticity $\{\langle\delta\omega^2(r)\rangle = \langle[\omega(r)-\omega(0)]^2\rangle\}$ are displayed in the insets to these figures. Their variation is consistent with the previous test but as mentioned above these structure functions are not strictly logarithmic. It should be noted here that this structure function looks similar to previously reported vorticity structure functions [4,16] (where particle tracking velocimetry was used).

We have studied two-dimensional turbulence both numerically (direct numerical simulations) and experimentally. While the experiments are limited by the small or moderate values of the Reynolds number, the simulations allow much higher Reynolds numbers. The results are in good agreement with theoretical expectations for the energy and scalar spectra as well as the energy transfer function. The vorticity correlation function is logarithmic according to our data. These results are consistent with already existing experiments and numerical simulations and extend them through tests of previously unmeasured quantities such as the energy transfer function, the scalar spectrum, and the vorticity correlation functions.

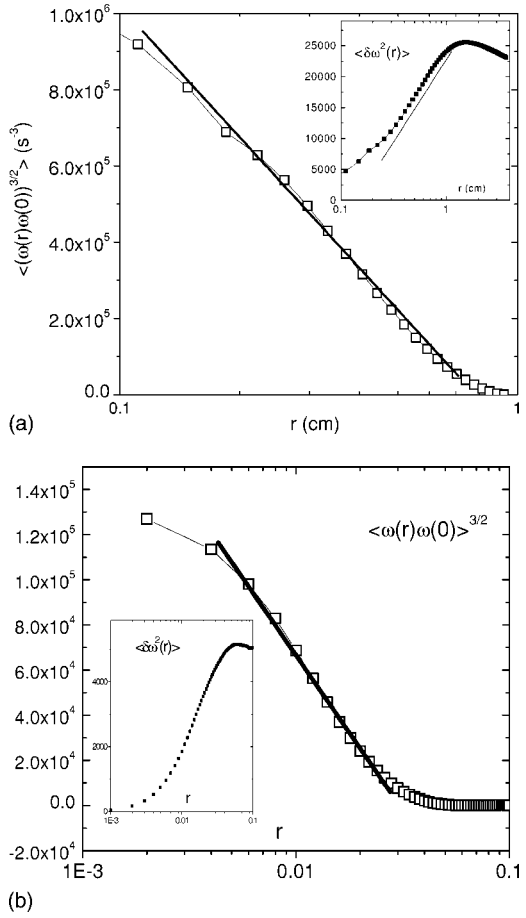

FIG. 5. $\langle\omega(0)\omega(r)\rangle^{3/2}$ versus r in semilog plot: (a) experiments; (b) numerical simulations. The insets show the vorticity structure functions.

[1] U. Frish, *Turbulence* (Cambridge University Press, Cambridge, U. K., 1995).

[2] R. Kraichnan, Phys. Fluids **10**, 1417 (1967); G. K. Batchelor, Phys. Fluids (Suppl.) **2**, 233 (1969).

[3] C. V. Tran and T. G. Shepherd, Physica D **165**, 199 (2002); C. V. Tran and J. C. Bowman, *ibid.* **176**, 242, (2003); Phys. Rev. E **69**, 036303 (2004).

[4] H. Kellay and W. I. Goldburg, Rep. Prog. Phys. **65**, 845 (2002).

[5] M. Rutgers, Phys. Rev. Lett. **81**, 2244 (1998).

[6] O. Greffier, Y. Amarouchene, and H. Kellay, Phys. Rev. Lett. **88**, 194101 (2002).

[7] A. Belmonte, B. Martin, and W. I. Goldburg, Phys. Fluids **12**, 835 (2000).

[8] C. H. Bruneau, O. Greffier, and H. Kellay, Phys. Rev. E **60**, R1162 (1999); H. Kellay, C. H. Bruneau, and X. L. Wu, Phys. Rev. Lett. **84**, 1669 (2000); Ph. Angot, C. H. Bruneau, and P. Fabrie, Numer. Math. **81**, 497 (1999); C. H. Bruneau and P. Fabrie, Math. Modell. Numer. Anal. **30**, 815 (1996); Int. J. Numer. Methods Fluids **19**, 693 (1994); C. H. Bruneau and C. Jouron, J. Comput. Phys. **89**, 389 (1990); C. H. Bruneau, Comput. Fluid Dyn. J. **1**, 114 (1998).

[9] H. Kellay, X. L. Wu, and W. I. Goldburg, Phys. Rev. Lett. **74**, 3975 (1995).

[10] V. Borue, Phys. Rev. Lett. **72**, 1475 (1994).

[11] G. Boffetta, A. Celani, and M. Vergassola, Phys. Rev. E **61**,

R29 (2000); E. Lindborg, J. Fluid Mech. **388**, 259 (1999).
[12] C. W. Van Atta (private communication). The derivation follows the same reasoning as in C. W. Van Atta and W. Y. Chen, J. Fluid Mech. **38**, 743 (1969); see also G. K. Batchelor, *The Theory of Homogeneous Turbulence* (Cambridge University Press, Cambridge, U. K., 1953).
[13] M. Lesieur, *Turbulence in Fluids* (Kluwer Academic, Dordrecht, 1990).
[14] Y. Amarouchene, and H. Kellay, Phys. Rev. Lett. **89**, 104502 (2002).
[15] G. Falkovich and V. Lebedev, Phys. Rev. E **49**, R1800 (1994).
[16] M. K. Rivera *et al.*, Phys. Rev. Lett. **90**, 104502 (2003).